

## Electronic Supplementary Information

### Manganese (III) porphyrin microbubbles for enhanced ultrasound/MR bimodal tumor imaging through ultrasound mediated micro-to-nano conversion

Min Chen,<sup>a</sup> Xiaolong Liang<sup>\*b</sup> and Zhifei Dai<sup>\*a</sup>

<sup>a</sup> Department of Biomedical Engineering, College of Engineering, Peking University, Beijing 100871, People's Republic of China. Email: [zhifei.dai@pku.edu.cn](mailto:zhifei.dai@pku.edu.cn) ;

<sup>b</sup> Department of Ultrasound, Peking University Third Hospital, Beijing 100191, People's Republic of China. Email: [xiaolong\\_liang2010@163.com](mailto:xiaolong_liang2010@163.com) ;

\* corresponding author

## Experimental Section

### Materials

Porphyrin grafted lipid (PGL) was synthesized according to previous report.<sup>1</sup> Dipalmitoyl-sn-glycero-3-phosphocholine (DSPC) and 1,2-distearoyl-snglycero-3-phosphoethanol amine-N-[methoxy(polyethyleneglycol)-2000](DSPE-PEG<sub>2000</sub>) were obtained from Shanghai A.V.T. Pharmaceutical Co., Ltd. MTT [3-(4,5- dimethylthiazol-2-yl)-2,5 -diphenyltetrazolium bromide] is a product of Sigma. All other reagents and solvents were purchased from domestic suppliers and used as received. Deionized (DI) water was obtained by a Milli-Q Water Purification system.

### Synthesis of MnP

Free PGL (15 mg, 9.39  $\mu$ mol) was dissolved in glacial AcOH, followed by addition of MnCl<sub>2</sub> (5.91 mg, 47  $\mu$ mol) and NaOAc (15.41mg, 188  $\mu$ mol). The mixture was heated to 120°C in a two-neck bottle for 8 hours with reflux. The reaction was monitored by ultraviolet-vision absorption spectrophotometer and the reaction was stopped when the peak at 419nm fully converted into the peak at 470nm indicating the full chelation of Mn onto PGL. The resulting solution was evaporated to remove the solvent and further purified by silica chromatography to get the dark green product.

### Synthesis of MnP-MBs

MnP (6.78 mg, 15 mol%) were dissolved in THF and mixed with 1,2-distearoyl-sn-glycero-3-phospho- choline (DSPC, 10.45 mg, 50 mol%), cholesterol (3.07 mg, 30 mol%), and 1,2-distearoyl-sn- glycero-3-phosphoethanolamine-N-[amino(polyethylene glycol)-2000] (DSPE-PEG<sub>2000</sub>, 3.70 mg, 5 mol%) dissolved in methanol. The mixture was added to deionized water in a 37°C water bath sonication accompanied by gentle shaking. The resulting

aqueous suspension was transferred to dialysis bag (8000–14000 Da) for 4 h to remove the excess organic solvents. The obtained MnP-NPs solution was transferred to a small vial by mixing with glycol and 1,2-propylene glycol at a molar ratio of 8:1:1. Then C<sub>3</sub>F<sub>8</sub> was introduced to the vial for 45 s to place the air within the vial and sealed carefully. A vial-mix mechanical agitator was employed to generate MBs by violent vibration for 45 s. The as prepared MnP-MBs can be handled by small injectors.

### **Characterizations**

Mass spectroscopy was tested by a Fourier transform ion cyclotron resonance mass spectrometer (Solarix XR, Bruker). UV-vis absorption spectra were measured by a UV-vis spectrophotometer (Thermo Fisher, Evolution 220). The morphology analysis of ultrasound induced MnP-MBs to MnP-NPs conversion was carried out by TEM (T20, FEI) by negative stained samples on cubic grid (200 mesh). Briefly, the as-prepared PCF-MBs solution was exposed to a 1.0 MHz ultrasound (1.0 W/cm<sup>2</sup>, 50% duty cycle) transducer for 5 min, then 10 μL of the resulting sample was dropped onto the grid, air-dried, and negatively stained with (10 μL, 3.0%) phosphotungstic acid followed by DI water washing and air-drying. Imaging was performed at an accelerating voltage of 200 kV. The concentration of the MnP-MBs was determined with a Coulter Counter Multisizer (Coulter Electronics Ltd., Luton, Bedfordshire, UK), in which 20 μL samples were diluted in 20 mL Isoton-II electrolyte solution. The ultrasound imaging of the MnP-MBs in solution was performed in a latex tube using a linear ultrasound imaging transducer (X4-12L, Vinno).

### **Ultrasound instrumentation**

The instrument employed for ultrasound microbubble destruction is a home-made instrument. A function signal generator (33220A, Agilent, USA), a power amplifier (2100L, E&I, USA), ultrasound transducer (H-107, Sonic Concept) was connected by coaxial cables (50 ohms) by sequence. The acoustic field can be measured by the hydrophone of a 3D positioning system (AIMS, ONDA, USA). Other transducer used in Fig. S3 are immersion transducer IL0.508HP and IL1.508HP purchased from Valpay Fisher.

### **In vitro ultrasound imaging investigation**

Different concentrations of MnP-MBs (0~8×10<sup>4</sup> MBs/ml) were prepared by diluting MnP-MBs with saline. 1ml of each dilution was first injected into a latex tube with mild agitation under a water bath beneath an ultrasound probe with a centre frequency of 5.0 MHz (Vinno). In order to monitor the ultrasound targeted microbubble destruction at different depth along the z axis, microbubbles were scattered under water, while the distance between the imaging plane and the therapeutic transducer was gradually adjusted from 2cm to 8 cm. The bubble disruption can take place at ultrasound exposure (1MHz, 50% duty cycle, 5s) where the black hole can indicate the successful microbubble disruption and the focal center of the ultrasound transducer.

### **In vitro and in vivo MR imaging**

For T1-weighted MR imaging, the following parameters were adopted: field of view (FOV) ¼ 40 mm 40 mm, matrix size ¼ 128 256, section thickness ¼ 2 mm, echo time (TE) ¼ 19 ms,

repetition time (TR)  $\frac{1}{4}$  520 ms, number of averages  $\frac{1}{4}$  3. The MR imaging of aqueous MnP-NPs and in vivo experiments were acquired by the Pharmascan 70/16 US In-vivo MRI system (Bruker, 7.0 T) with the parameters TR  $\frac{1}{4}$  1000 ms; TE  $\frac{1}{4}$  9 ms. MRI data sets were first acquired to serve as baseline controls before injection, and then animals were rescanned 30 min, 1h, 3h, 6h, 8h and 24 h post-injection. For animal imaging, nude mice bearing U87 tumor were first anesthetized and then intravenously injected with aqueous MnP-MBs (or MnP-NPs) (dose: 100  $\mu$ L, 2 mg /mL).

### **MTT assay**

The number of live cells is directly proportional to the absorbance of formazan at 570 nm (produced in living cells by the cleavage of MTT by dehydrogenases). Briefly, solution of MTT in sterile PBS were prepared with a concentration of 5 mg/mL, and 20 mL was added to each well and incubated for another 4 h at 37 °C with 5% CO<sub>2</sub>. Next, the medium was carefully removed and 150 mL of DMSO was added into the well. Then the absorbance at 490 nm was measured using a microplate reader (Synergy HT, BioTek ). Cells incubated with serum-supplemented medium represent 100% cell survival. Each concentration and light dose were run in five replicate wells, and each experiment was repeated for three times.

### **Animal model setup**

In vivo Animal Models and Treatments. The animal experiment protocols were approved by Peking University Institutional Animal Care and Use Committee (IACUC). In vivo experiments were carried out on 4-week-old male Balb/c nude mice weighing 20–22 g (Beijing Vital River Laboratory Animal Technology Co., Ltd.). For tumor inoculations, animals were inhalation anesthetized with isoflurane. Subcutaneous tumors were implanted by injection of a volume of 100  $\mu$ L cell suspension containing  $5 \times 10^6$  U87 glioma cancer cells implanted on the right hind leg. Ten days after cancer cell implantation, the volumes of the subcutaneous tumors reached about 200 mm<sup>3</sup>, the in vivo experiments were started. U87 glioma tumor-bearing mice were randomly divided into 3 groups (n = 3), then intravenously injected via tail vein with MnP-MBs, or MnP-NPs at a Mn injection dose of 0.09mg (1.65  $\mu$ mol ) /kg. MnP-MBs group received ultrasound exposure on the tumor site under the guidance of CEUS, with a pulse low intensity ultrasound (1MHz, 50% duty cycle) treatment for 3min.

### **Reference**

1. Liang X, Li X, Jing L, et al. Theranostic porphyrin dyad nanoparticles for magnetic resonance imaging guided photodynamic therapy, *Biomaterials*, 2014, 35(24): 6379-6388.

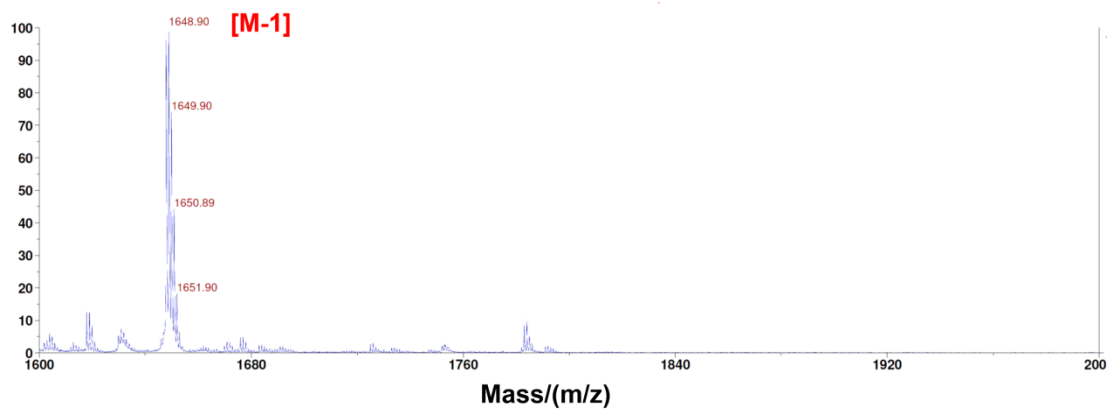


**Fig. S1 Mass spectrum of MnPGL** shows the molecular ion peak of [M-1] at 1648.90 indicating the successful chelation of Mn to PGL.

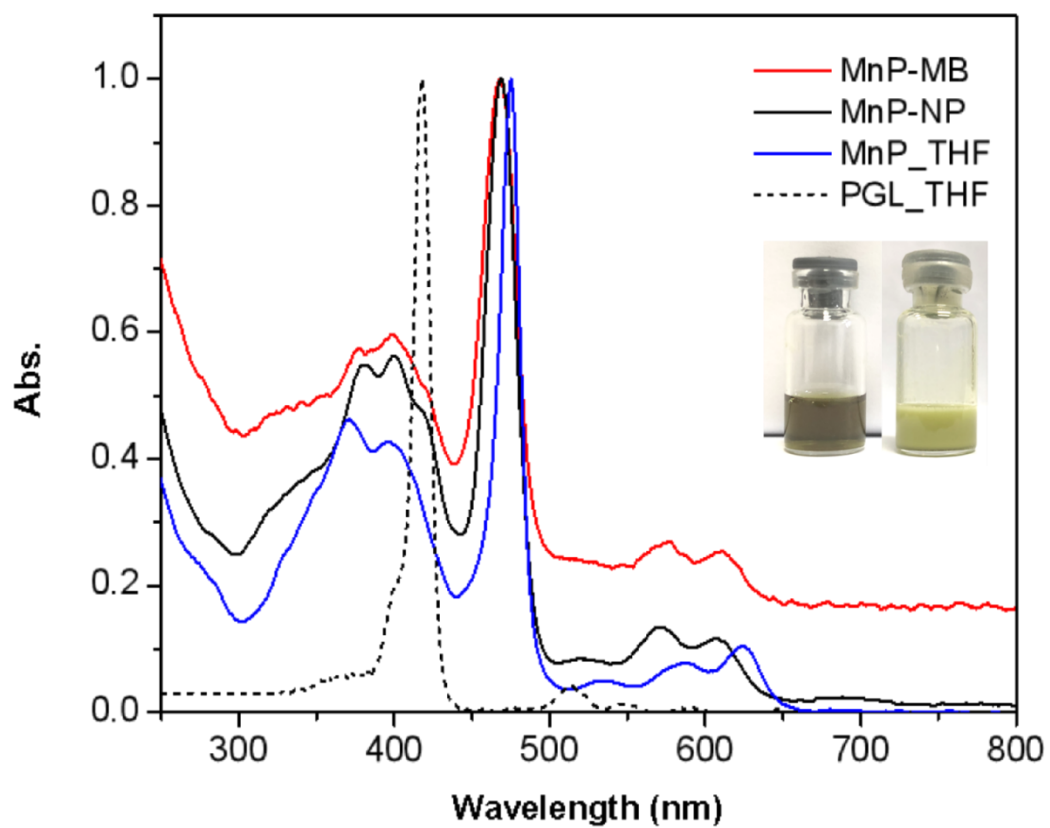


**Fig. S2 UV-vis absorption spectra of MnP-MBs and MnP-NPs aqueous solutions**

While MnP and PGL were dissolved in organic solvents were used as controls. The characteristic absorption peak of tetra-pyrrole shifted from 415nm to 470nm after Mn chelation.

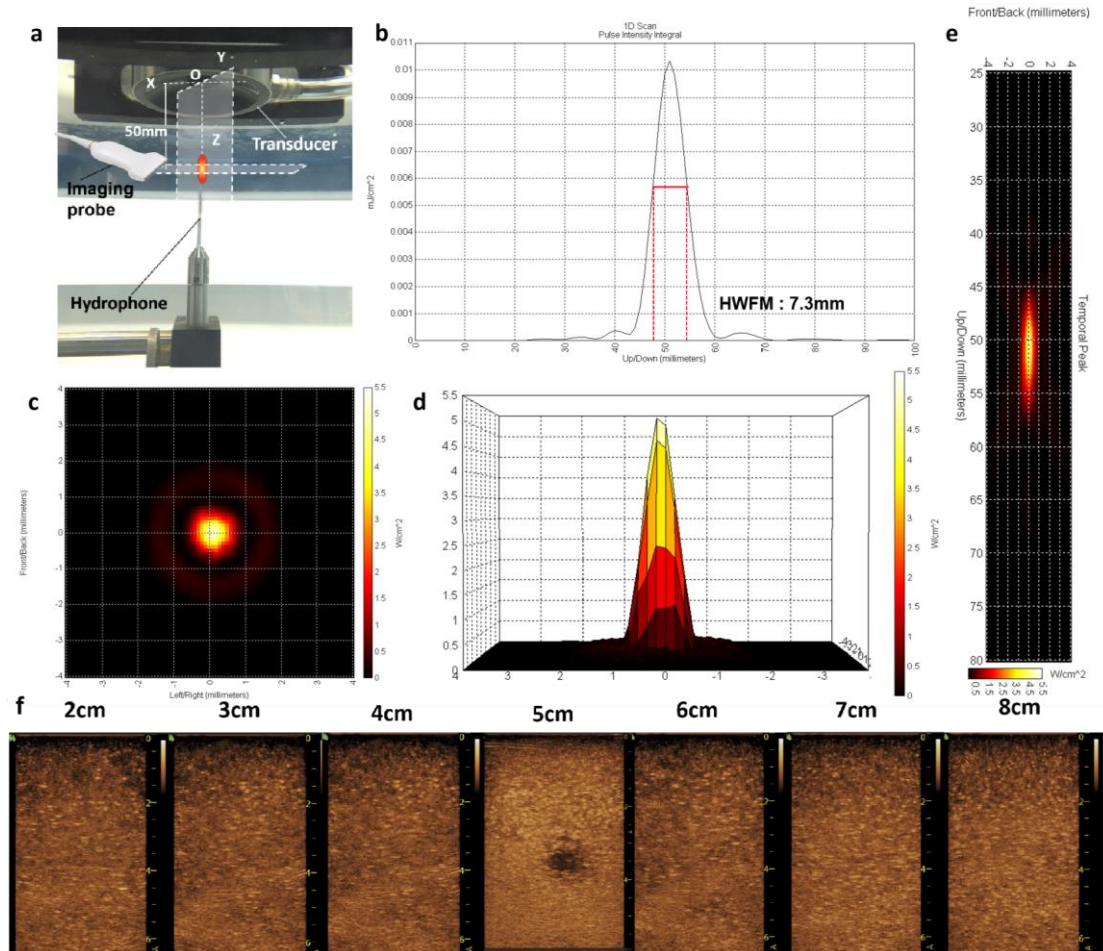


**Fig. S3 Quantification of the acoustic field of the ultrasound transducer used for UTMD.** (a) Set-up of the 3D acoustic field measuring system, (b) 1D scan of the intensity along the z axis of the transducer, 2D scan of XY plane at the distance of 50mm from the OZ axis(c) and its surface plot(d), 2D scan of YOZ plane(e) indicates the focal center lies 50mm beneath the center of the transducer, (f) monitoring of ultrasound targeted microbubble destruction was carried out by place an imaging probe parallel to the XOY plane at different depths from 2cm to 8cm and the bubble disruption can take place at ultrasound exposure (1MHz, 50% duty cycle, 5s) where the black hole at 5cm indicate the successful microbubble disruption and focal center.

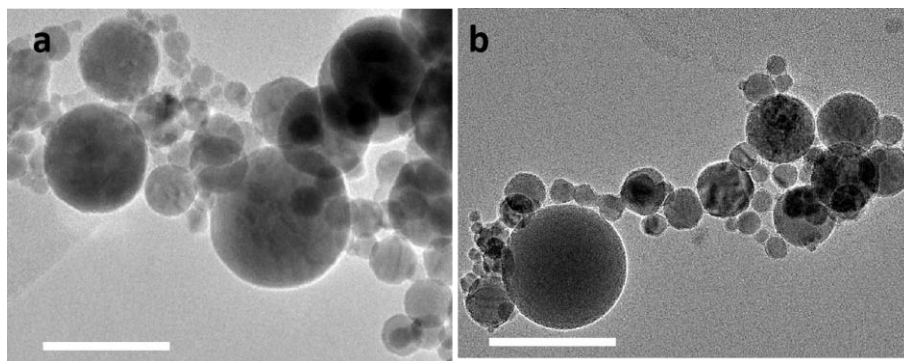


**Fig. S4 TEM images of MnP-NPs converted from MnP-MB** by ultrasound transducers with different center frequencies. (a) 0.5MHz, (b)1.5MHz (scale bar: 100nm)

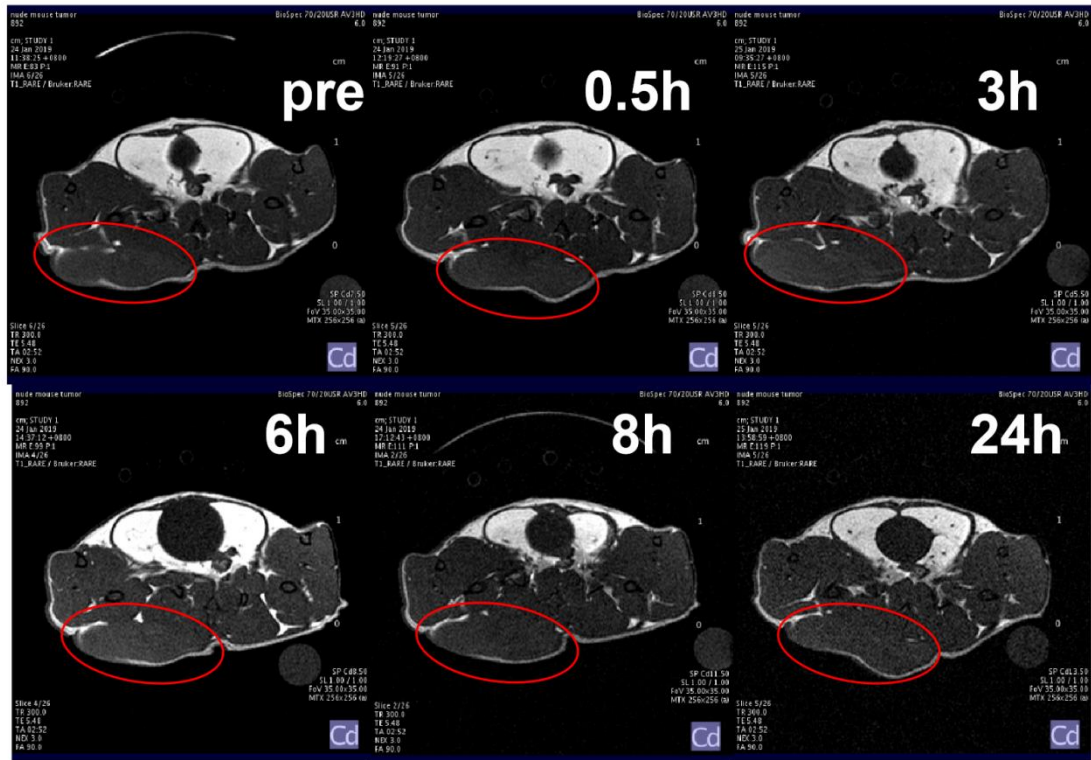


**Fig. S5** The MRI images of mouse before and after MnP-NPs intravenously injection, which shows no significant contrast enhancement.

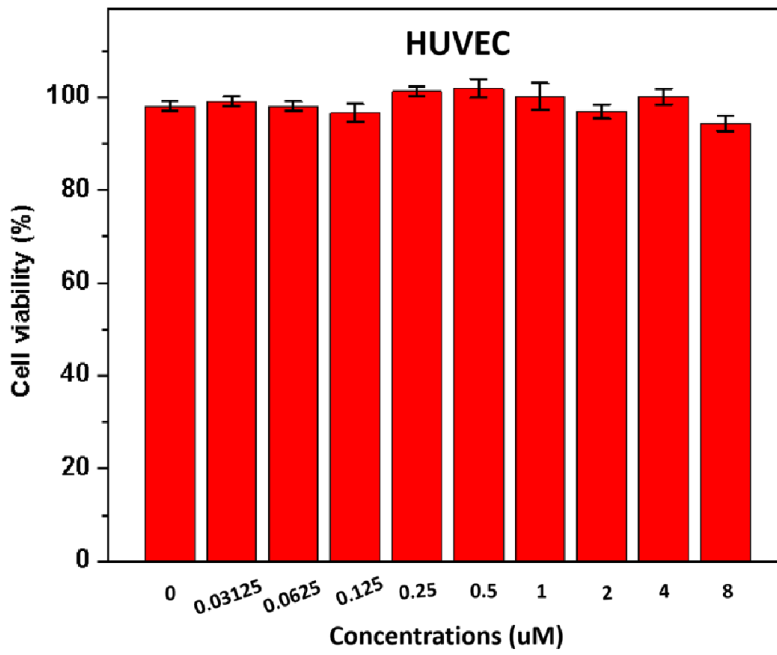
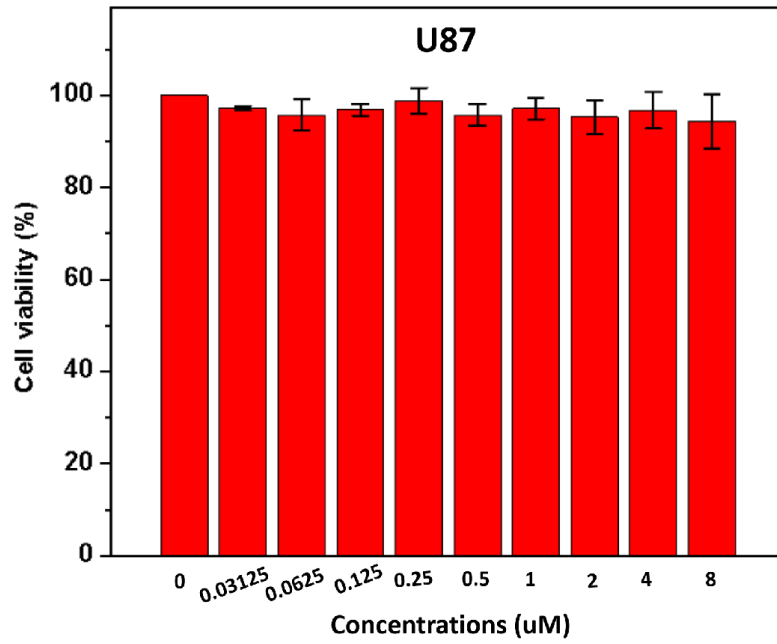


**Fig. S6 Cytotoxicity of MnP-MBs to U87 glioma cancer cells and human umbilical vein endothelial cells (HUVEC) after incubation for 48h.**